genome in nonneuronal cells, similar to the apparent protection of LAT-promoter activity in latently infected sensory neurons.

A critical limitation of most existing replication-defective HSV vectors is the presence of one or more expressed IE genes that are activated on infection in a manner independent of other viral-gene expression. ICP0 expression has proved especially important for transgene activity because the elimination of ICP0 activity led to complete genome silencing (13, 16). Although ICP0 has the attractive feature of preventing heterochromatin remodeling and consequent transgene silencing (15), it can also induce cell-cycle arrest in dividing cells and apoptosis in postmitotic cells (18, 31). To overcome this problem, HSV vectors have been engineered to dramatically reduce but not eliminate ICP0 expression in the hope that low levels of the protein would maintain transgene activity without loss of cell proliferation or viability (8, 9, 17, 32). However, these strategies do not universally eliminate vector toxicity for nonneuronal cells, which varies with the target cell and multiplicity (7, 11). Our study confirms that even low levels of ICP0 can reduce cell viability despite the upside of maintaining some transgene expression. This reduced viability may be a result of the action of ICP0 alone or possibly in combination with leaky expression of other viral functions. Thus, we and others have searched for a strategy to express transgenes when all IE gene expression is shut down.

In one approach to achieve this goal, ICP0 has been substituted with similar IE genes from other herpesviruses, including the pp71 gene of human cytomegalovirus (HCMV) (33, 34), a betaherpesvirus, with the notion that the products of these genes may provide the antisilencing functions of ICP0 without toxicity (35). However, it is well-known that pp71 degrades a chromatin-remodeling factor, hDaxx, followed by disruption of the hDaxx–ATRX complex (36, 37) and members of the retinoblastoma tumor-suppressor family of proteins (38). The disruption of the hDaxx–ATRX complex can cause genomic instability (39) whereas the loss of retinoblastoma family proteins dysregulates normal cell-cycle progression (40, 41). Indeed, pp71 overexpression seems to induce malignant alteration of the cell. Everett et al. have used an inducible cell-line system to demonstrate that the ICP0 equivalents of the alphaherpesviruses, bovine herpes virus type 1 (BHV-1), equine herpesvirus type 1 (EHV-1), and pseudorabies virus (PRV), can effectively derepress silent HSV-1 genomes (42). However, they also reported that all three of these proteins adversely affect cell growth, although less dramatically than ICP0. Thus, prior results argue that the strategies of reducing ICP0 expression or substituting ICP0 with other herpesvirus transactivators will not solve the problem of genome silencing in the absence of ICP0 without deleterious effects on the cells.

Because the latency locus remains active in neuronal cells at a time when all viral lytic genes are silenced, including the ICP0 gene, we and others reasoned that this locus might be a preferred site for transgene expression from quiescent HSV genomes in nonneuronal cells. Lilley et al. (32) used a highly debilitated vector to demonstrate reporter-gene expression in Vero cells at 23 dpi from a LATP2-linked expression cassette in the UL41 locus, but residual ICP0 expression could not be ruled out. Our results show that a foreign promoter inserted into the LAT locus can drive robust short-term reporter-gene expression in the complete absence of IE gene products in a variety of primary human nonneuronal cells and that this expression can persist in postmitotic cells. These attributes of our platform create a gene-transfer vector with broad utility beyond the nervous system. We proceeded to examine which elements within the LAT locus provided for this remarkable transgene expression.

Recent findings have shown that, during latency, the cellular CTCF protein is enriched on the two HSV CTRLs and that acetylated histone H3, an epigenetic beacon of active transcription, accumulates in the LAT region between these elements (19, 43–45). These findings suggested that CTRLs may act as boundary elements to shield the LAT locus against the spreading of repressive epigenetic modifications (29), and it was shown in short-term plasmid transfection assays that a fragment encompassing CTRL2 combines the functions of a typical insulator (19). In the context of a complete viral genome, we found that CTRL1, along with LATP2, was essential for preventing the rapid silencing of an ectopic promoter in the LAT locus in nonneuronal cells in the absence of all viral IE gene products (Fig. 3). Furthermore, we showed that the LAT locus provides protection against the silencing of an embedded promoter when moved away from its native position in the viral genome (Fig. 4) and supports long-term expression in postmitotic human fibroblasts (Figs. 2*D* and 6*C*) and striatal muscle cells (Fig. 5*C*). CTRL1 consists of 46 copies of two separate, but overlapping, CTCF-binding motifs whereas CTRL2 contains 9 copies of only one of these motifs (19), perhaps explaining the greater effect of CTRL1 than CTRL2 deletion on transgene expression in the LAT locus. Recent evidence indicates that the function of insulators is dependent on additional sequences aside from CTCF-binding motifs, and thus a more complete analysis of these viral elements will be required to determine whether they have specific limitations (46). LAP2 (LATP2) has been reported to contain chromatin-binding elements that bend DNA, and such activity could enhance the function of nearby foreign promoters (47). Although some chromatin regulatory elements located within the LAT promoter regions have shown tissue specificity, it has been unclear whether LATP2 can be broadly useful to counteract transgene silencing in nonneuronal cells in the absence of ICP0 (48, 49). Our data indicate that, in combination with CTRL1 and to a lesser extent alone, it can.

We used a ubiquitin C promoter-mCherry cassette in the ICP4 locus to monitor the effect of sequential deletion of IE genes on transgene expression. As expected, expression in HDFs declined to essentially undetectable with the progressive removal of all IE gene functions, but we could readily detect mCherry fluorescence during growth of the different vectors in complementing cells, as well as on infection of unmodified U2OS cells. These findings were consistent with the designs of the sequential JΔNI backbones, and mCherry expression from JΔNI5 derivatives was not demonstrably altered or elevated in other noncomplementing cells, with one notable exception, DRG neurons. Although we do not yet know the cause of this difference, a recent report by Harkness et al. noted greater persistence of transcriptional activity within repeat regions of the IE gene-depleted *d*109 vector than elsewhere along the genome in trigeminal ganglion neurons, but not in MRC5 human embryonic lung cells (50). The mCherry cassette in our vectors replaces the ICP4 gene in the remaining repeat bordering U_S, a region flanked on each side by a cluster of CTCF-binding motifs referred to by Bloom and coworkers as CTa_S (or B4) and CTRS3′ (or B6), respectively (19, 29). Because the ICP4 gene is severely repressed in latently infected neurons relative to the LAT region, it seems unlikely that these elements alone are responsible for the enhanced mCherry expression we observed in rat DRGs, and thus other factors, including the nature of the transgene promoter, may play an important role.

The application of highly defective HSV vectors for gene therapy will require methods for efficient vector engineering and subsequent production minimizing defective particles. We found that our highly defective vectors can be readily produced as infectious particles by transfection of the corresponding BAC constructs into complementing U2OS-ICP4/27 cells and can be amplified to high titers on these cells (Table 2). Importantly, because there is no sequence overlap between the complementing genes in U2OS-ICP4/27 cells and the genome of JΔNI5 and its derivatives, the risk of generating replication-competent revertants is minimal. We used U2OS cells for vector complementation because these cells naturally complement ICP0 function (21), thus

eliminating the need to express this toxic protein. In the past, Vero cells engineered to complement ICP0 in addition to ICP4 and ICP27 have proven difficult to maintain (10) whereas our U2OS-ICP4/27 line is stable. Moreover, we found that U2OS cells can tolerate constitutive expression of ICP4 whereas the kinetics of ICP4 induction in Vero-based cells in response to defective virus infection can be slow (51). We have also added Cre recombinase to our complementing line to eliminate the BAC region during vector production. Removal of the 11-kb BAC insert had the advantage of recreating space for recombinant sequences and eliminating residual JΔNI5 toxicity for HDFs. Although bacterial sequences have been shown to contribute to transgene silencing in different vector systems (52), we observed only a modest increase in long-term reporter-gene expression as a result of BAC excision. It is also noteworthy that none of our BAC vector constructs challenged the size limit for efficient viral-genome packaging into virions, suggesting that the consistent growth acceleration we have noticed after BAC excision is due to other factors, perhaps including the elimination of possible recognition of the bacterial sequences by pattern-recognition receptors such as TLR9. Together, our U2OS-ICP4/27-Cre and U2OS-ICP4/27 cells provide an effective and reliable means to produce safe stocks of highly defective HSV vectors from engineered BAC constructs, important attributes for application to patient therapies.

In summary, we describe for the first time, to our knowledge, a nontoxic HSV-vector platform that can accommodate large transgenes, exemplified by the 14-kb mouse dystrophin cDNA, with continued expression in nonneuronal cells. Our results indicate that proximity to certain elements from the LAT locus protects transgene expression against viral-genome silencing. This new generation of HSV vector represents a potent tool for delivery of large payloads to both neuronal and nonneuronal cells, suggesting that it will fill an important niche in the gene-therapy vector arsenal.

Materials and Methods

Cells. Human osteosarcoma U2OS cells (ATCC) were grown in DMEM with 10% (vol/vol) FBS and penicillin-streptomycin (P/S). HDFs (PCS-201-010; ATCC) and BJ human foreskin fibroblasts (CRL-2522; ATCC) were grown in DMEM with 10% (vol/vol) Embryonic Stem Cell Qualified FBS (Invitrogen) and P/S. Vero, Vero-7b (7), and 293T cells were cultured in DMEM containing 5% (vol/vol) FBS and P/S. hHEPs were isolated and cultured as described (53, 54). hPADs (PT-5020; Lonza) were maintained with PBM-2 Basal Medium (Lonza). hMDSCs (kindly provided by J. Huard, University of Pittsburgh, Pittsburgh, PA) were cultured as described (55). hEKs (Invitrogen) were cultured in EpiLife Medium supplemented with Human Keratinocyte Growth Supplement (both from Invitrogen). DRGs were microdissected from day-15 rat embryos, dissociated with 3 mg/mL type-I collagenase (Sigma) in Leibovitz's L-15 media for 30 min at 37 °C with constant shaking, and plated on poly-D-lysine (Sigma)–coated coverslips at ~10^5 cells per well in 24-well plates in 500 μL of defined Neurobasal medium with B27 supplement, Glutamax-I, Albumax-II, and P/S (Gibco/Invitrogen), supplemented with 100 ng/mL 7.0S NGF (Sigma). At 1–3 d post-plating, cultures were treated with 10 μM uridine and 10 μM fluorodeoxyuridine (Sigma) in the above media for 1–2 d to limit the expansion of dividing cells, such as fibroblasts and glia. Cells were then washed with PBS and incubated with NGF-supplemented Neurobasal medium as above. Virus infections were performed at 10–15 d after plating. Differentiation-prone muscle progenitor cells from dystrophin-deficient *mdx* mice (kindly provided by J. Huard and B. Wang, University of Pittsburgh, Pittsburgh, PA) were isolated and cultured as described (56).

U2OS-ICP4 cells (**Fig. S1*A***) were generated by infection of U2OS cells with purified ICP4 lentivirus as described in ***SI Materials and Methods***. Puromycin (2 μg/mL)-resistant clones were isolated and screened by infection with ICP4-deficient virus (QOZHG) at a multiplicity of infection (MOI) of 0.5 before immunofluorescent staining for ICP4. U2OS-ICP4/27 cells were similarly generated by infection of U2OS-ICP4 cells with purified ICP27 lentivirus, selection for resistance to puromycin (2 μg/mL) and blasticidin (10 μg/mL), and screening of QOZHG-infected clones for ICP27 immunofluorescence. We tested the stability of the JΔNI5-complementing properties of the U2OS-ICP4/27 clone used in this study by plaque assay at different cell passages and found no significant decline in plaquing efficiency through at least 20 passages (**Table S1**).

Additional materials and methods are provided in ***SI Materials and Methods*** and **Tables S2** and **S3**.

ACKNOWLEDGMENTS. We are grateful to Hiroyuki Nakai for the pBluescriptUB-Flag-mArt plasmid; Klaus Osterrieder for plasmids pEPkan-S2 and pBAD-*I-sceI*; J. Thomson (Morgridge Institute) for pEP4-EO2SCK2M-EN2L (Addgene plasmid 20924); Greg Smith for *Escherichia coli* strain GS1783; David Leib for KOS37-BAC DNA; Tsuyoshi Akagi for pCX4hyg; Nobutaka Kiyokawa, Hajime Okita and Akihiro Umezawa for retroviral packaging plasmids; Patricia Spear for pPEP100; John Blaho for anti-ICP22; T. J. Ley (Washington University) for pTurbo-Cre; Thomas Caskey for pCCL-DMD; Johnny Huard and Bing Wang for hMDSCs and *mdx* muscle progenitor cells; and Mingdi Zhang for rat DRG culturing. This work was supported by NIH Grants NS064988 and DK044935, CHDI Foundation Grant A3777, and Commonwealth of Pennsylvania Grant SAP 4100061184 (to J.C.G.). P.M. was supported by an Atlante fellowship from the University of Ferrara, Italy, under the mentorship of Michele Simonato. G.V. was supported by a grant from the Italian Ministry for University and Research (PRIN 2010-11 2010N8PBAA) (to Michele Simonato).

1. Thomas CE, Ehrhardt A, Kay MA (2003) Progress and problems with the use of viral vectors for gene therapy. *Nat Rev Genet* 4(5):346–358.
2. Allocca M, et al. (2008) Serotype-dependent packaging of large genes in adeno-associated viral vectors results in effective gene delivery in mice. *J Clin Invest* 118(5):1955–1964.
3. Fairclough RJ, Wood MJ, Davies KE (2013) Therapy for Duchenne muscular dystrophy: Renewed optimism from genetic approaches. *Nat Rev Genet* 14(6):373–378.
4. Monahan PE, et al. (2010) Proteasome inhibitors enhance gene delivery by AAV virus vectors expressing large genomes in hemophilia mouse and dog models: A strategy for broad clinical application. *Mol Ther* 18(11):1907–1916.
5. Krisky DM, et al. (1997) Rapid method for construction of recombinant HSV gene transfer vectors. *Gene Ther* 4(10):1120–1125.
6. Krisky DM, et al. (1998) Development of herpes simplex virus replication-defective multigene vectors for combination gene therapy applications. *Gene Ther* 5(11):1517–1530.
7. Krisky DM, et al. (1998) Deletion of multiple immediate-early genes from herpes simplex virus reduces cytotoxicity and permits long-term gene expression in neurons. *Gene Ther* 5(12):1593–1603.
8. Palmer JA, et al. (2000) Development and optimization of herpes simplex virus vectors for multiple long-term gene delivery to the peripheral nervous system. *J Virol* 74(12): 5604–5618.
9. Preston CM, Mabbs R, Nicholl MJ (1997) Construction and characterization of herpes simplex virus type 1 mutants with conditional defects in immediate early gene expression. *Virology* 229(1):228–239.
10. Samaniego LA, Wu N, DeLuca NA (1997) The herpes simplex virus immediate-early protein ICP0 affects transcription from the viral genome and infected-cell survival in the absence of ICP4 and ICP27. *J Virol* 71(6):4614–4625.
11. Wu N, Watkins SC, Schaffer PA, DeLuca NA (1996) Prolonged gene expression and cell survival after infection by a herpes simplex virus mutant defective in the immediate-early genes encoding ICP4, ICP27, and ICP22. *J Virol* 70(9):6358–6369.
12. Jackson SA, DeLuca NA (2003) Relationship of herpes simplex virus genome configuration to productive and persistent infections. *Proc Natl Acad Sci USA* 100(13):7871–7876.
13. Samaniego LA, Neiderhiser L, DeLuca NA (1998) Persistence and expression of the herpes simplex virus genome in the absence of immediate-early proteins. *J Virol* 72(4): 3307–3320.
14. Terry-Allison T, Smith CA, DeLuca NA (2007) Relaxed repression of herpes simplex virus type 1 genomes in Murine trigeminal neurons. *J Virol* 81(22):12394–12405.
15. Ferenczy MW, DeLuca NA (2011) Reversal of heterochromatic silencing of quiescent herpes simplex virus type 1 by ICP0. *J Virol* 85(7):3424–3435.
16. Ferenczy MW, Ranayhossaini DJ, Deluca NA (2011) Activities of ICP0 involved in the reversal of silencing of quiescent herpes simplex virus 1. *J Virol* 85(10):4993–5002.
17. Craft AM, et al. (2008) Herpes simplex virus-mediated expression of Pax3 and MyoD in embryoid bodies results in lineage-Related alterations in gene expression profiles. *Stem Cells* 26(12):3119–3129.
18. Hobbs WE, 2nd, DeLuca NA (1999) Perturbation of cell cycle progression and cellular gene expression as a function of herpes simplex virus ICP0. *J Virol* 73(10):8245–8255.
19. Amelio AL, McAnany PK, Bloom DC (2006) A chromatin insulator-like element in the herpes simplex virus type 1 latency-associated transcript region binds CCCTC-binding factor and displays enhancer-blocking and silencing activities. *J Virol* 80(5):2358–2368.
20. Tischer BK, von Einem J, Kaufer B, Osterrieder N (2006) Two-step red-mediated recombination for versatile high-efficiency markerless DNA manipulation in Escherichia coli. *Biotechniques* 40(2):191–197.
21. Yao F, Schaffer PA (1995) An activity specified by the osteosarcoma line U2OS can substitute functionally for ICP0, a major regulatory protein of herpes simplex virus type 1. *J Virol* 69(10):6249–6258.
22. Uchida H, et al. (2010) A double mutation in glycoprotein gB compensates for ineffective gD-dependent initiation of herpes simplex virus type 1 infection. *J Virol* 84(23):12200–12209.
23. Chen Xp, et al. (2000) Herpes simplex virus type 1 ICP0 protein does not accumulate in the nucleus of primary neurons in culture. *J Virol* 74(21):10132–10141.

24. Baines JD, Roizman B (1991) The open reading frames UL3, UL4, UL10, and UL16 are dispensable for the replication of herpes simplex virus 1 in cell culture. *J Virol* 65(2): 938–944.
25. Menotti L, Casadio R, Bertucci C, Lopez M, Campadelli-Fiume G (2002) Substitution in the murine nectin1 receptor of a single conserved amino acid at a position distal from the herpes simplex virus gD binding site confers high-affinity binding to gD. *J Virol* 76(11):5463–5471.
26. Goins WF, et al. (1994) A novel latency-active promoter is contained within the herpes simplex virus type 1 UL flanking repeats. *J Virol* 68(4):2239–2252.
27. Zwaagstra JC, Ghiasi H, Nesburn AB, Wechsler SL (1991) Identification of a major regulatory sequence in the latency associated transcript (LAT) promoter of herpes simplex virus type 1 (HSV-1). *Virology* 182(1):287–297.
28. Berthomme H, Lokensgard J, Yang L, Margolis T, Feldman LT (2000) Evidence for a bidirectional element located downstream from the herpes simplex virus type 1 latency-associated promoter that increases its activity during latency. *J Virol* 74(8): 3613–3622.
29. Bloom DC, Giordani NV, Kwiatkowski DL (2010) Epigenetic regulation of latent HSV-1 gene expression. *Biochim Biophys Acta* 1799(3-4):246–256.
30. Pichavant C, et al. (2011) Current status of pharmaceutical and genetic therapeutic approaches to treat DMD. *Mol Ther* 19(5):830–840.
31. Sanfilippo CM, Blaho JA (2006) ICP0 gene expression is a herpes simplex virus type 1 apoptotic trigger. *J Virol* 80(14):6810–6821.
32. Lilley CE, et al. (2001) Multiple immediate-early gene-deficient herpes simplex virus vectors allowing efficient gene delivery to neurons in culture and widespread gene delivery to the central nervous system in vivo. *J Virol* 75(9):4343–4356.
33. Homer EG, Rinaldi A, Nicholl MJ, Preston CM (1999) Activation of herpesvirus gene expression by the human cytomegalovirus protein pp71. *J Virol* 73(10):8512–8518.
34. Preston CM, Nicholl MJ (2005) Human cytomegalovirus tegument protein pp71 directs long-term gene expression from quiescent herpes simplex virus genomes. *J Virol* 79(1):525–535.
35. Preston CM, Rinaldi A, Nicholl MJ (1998) Herpes simplex virus type 1 immediate early gene expression is stimulated by inhibition of protein synthesis. *J Gen Virol* 79(Pt 1): 117–124.
36. Lukashchuk V, McFarlane S, Everett RD, Preston CM (2008) Human cytomegalovirus protein pp71 displaces the chromatin-associated factor ATRX from nuclear domain 10 at early stages of infection. *J Virol* 82(24):12543–12554.
37. Saffert RT, Kalejta RF (2006) Inactivating a cellular intrinsic immune defense mediated by Daxx is the mechanism through which the human cytomegalovirus pp71 protein stimulates viral immediate-early gene expression. *J Virol* 80(8):3863–3871.
38. Kalejta RF, Bechtel JT, Shenk T (2003) Human cytomegalovirus pp71 stimulates cell cycle progression by inducing the proteasome-dependent degradation of the retinoblastoma family of tumor suppressors. *Mol Cell Biol* 23(6):1885–1895.
39. De La Fuente R, Baumann C, Viveiros MM (2011) Role of ATRX in chromatin structure and function: Implications for chromosome instability and human disease. *Reproduction* 142(2):221–234.
40. Dannenberg JH, van Rossum A, Schuijff L, te Riele H (2000) Ablation of the retinoblastoma gene family deregulates G(1) control causing immortalization and increased cell turnover under growth-restricting conditions. *Genes Dev* 14(23):3051–3064.
41. Sage J, et al. (2000) Targeted disruption of the three Rb-related genes leads to loss of G(1) control and immortalization. *Genes Dev* 14(23):3037–3050.
42. Everett RD, Boutell C, McNair C, Grant L, Orr A (2010) Comparison of the biological and biochemical activities of several members of the alphaherpesvirus ICP0 family of proteins. *J Virol* 84(7):3476–3487.
43. Ertel MK, Cammarata AL, Hron RJ, Neumann DM (2012) CTCF occupation of the herpes simplex virus 1 genome is disrupted at early times postreactivation in a transcription-dependent manner. *J Virol* 86(23):12741–12759.
44. Kubat NJ, Tran RK, McAnany P, Bloom DC (2004) Specific histone tail modification and not DNA methylation is a determinant of herpes simplex virus type 1 latent gene expression. *J Virol* 78(3):1139–1149.
45. Wang QY, et al. (2005) Herpesviral latency-associated transcript gene promotes assembly of heterochromatin on viral lytic-gene promoters in latent infection. *Proc Natl Acad Sci USA* 102(44):16055–16059.
46. Recillas-Targa F, Valadez-Graham V, Farrell CM (2004) Prospects and implications of using chromatin insulators in gene therapy and transgenesis. *BioEssays* 26(7):796–807.
47. French SW, Schmidt MC, Glorioso JC (1996) Involvement of a high-mobility-group protein in the transcriptional activity of herpes simplex virus latency-active promoter 2. *Mol Cell Biol* 16(10):5393–5399.
48. Emery DW, Chen H, Li Q, Stamatoyannopoulos G (1998) Development of a condensed locus control region cassette and testing in retrovirus vectors for A gamma-globin. *Blood Cells Mol Dis* 24(3):322–339.
49. Sadelain M, Wang CH, Antoniou M, Grosveld F, Mulligan RC (1995) Generation of a high-titer retroviral vector capable of expressing high levels of the human beta-globin gene. *Proc Natl Acad Sci USA* 92(15):6728–6732.
50. Harkness JM, Kader M, DeLuca NA (2014) Transcription of the herpes simplex virus 1 genome during productive and quiescent infection of neuronal and nonneuronal cells. *J Virol* 88(12):6847–6861.
51. Grant KG, Krisky DM, Ataai MM, Glorioso JC, 3rd (2009) Engineering cell lines for production of replication defective HSV-1 gene therapy vectors. *Biotechnol Bioeng* 102(4):1087–1097.
52. Suzuki M, Kasai K, Saeki Y (2006) Plasmid DNA sequences present in conventional herpes simplex virus amplicon vectors cause rapid transgene silencing by forming inactive chromatin. *J Virol* 80(7):3293–3300.
53. Ueki S, et al. (2011) Hepatic B7 homolog 1 expression is essential for controlling cold ischemia/reperfusion injury after mouse liver transplantation. *Hepatology* 54(1): 216–228.
54. Yoshida O, et al. (2013) CD39 expression by hepatic myeloid dendritic cells attenuates inflammation in liver transplant ischemia-reperfusion injury in mice. *Hepatology* 58(6):2163–2175.
55. Gao X, et al. (2013) BMP2 is superior to BMP4 for promoting human muscle-derived stem cell-mediated bone regeneration in a critical-sized calvarial defect model. *Cell Transplant* 22(12):2393–2408.
56. Gharaibeh B, et al. (2008) Isolation of a slowly adhering cell fraction containing stem cells from murine skeletal muscle by the preplate technique. *Nat Protoc* 3(9):1501–1509.
57. Gierasch WW, et al. (2006) Construction and characterization of bacterial artificial chromosomes containing HSV-1 strains 17 and KOS. *J Virol Methods* 135(2):197–206.

Supporting Information

Miyagawa et al. 10.1073/pnas.1423556112

SI Materials and Methods

Lentiviruses. Lentiviral ICP4 expression plasmid pCDH-ICP4-puro was constructed by replacing the complete HCMV IE promoter of plasmid pCDH-CMV-MCS-EF1-Puro (Systembio) with the ICP4 promoter and coding region from plasmid S3 containing the SphI fragment from pICP4-lox-pac (1) (GenBank JQ673480.1 HSV-1 KOS, map positions 131,587–124,379) in the SphI site of pUC19. Lentiviral ICP27 expression plasmid pCDH-ICP27-blast was constructed, first, by replacement of the puromycin-resistance cassette of pCDH-CMV-MCS-EF1-Puro with the blasticidin-resistance cassette of pcDNA6/BioEase-DEST (Invitrogen) to create pCDH-CMV-MCS-SV40-blast. The ICP27 promoter and coding region were then isolated by digestion of plasmid PD7 containing the ICP27 gene and flanking sequences between EcoRV and SacI sites (GenBank JQ673480.1, map positions 110,580–115,666) with BamHI (map position 113,244) and SacI, and the isolated fragment was used to replace the CMV promoter in pCDH-CMV-MCS-SV40-blast.

Lentiviruses were produced using the ViraPower Lentiviral Packaging Mix (Invitrogen) according to the manufacturer's instructions. Briefly, 293T cells were transfected with pCDH-ICP4-puro or pCDH-ICP27-blast in ViraPower mix. Supernatants were harvested 2 d later, clarified, filtered through a 0.45-μm filter, and concentrated by centrifugation.

HSV–BAC Recombineering. All HSV–BAC constructs generated in this study and converted to virus particles are listed in Table 1 and were derived from KOS-37 BAC (2), a kind gift from D. Leib (Dartmouth Medical School, Hanover, NH). All BAC engineering was performed by scarless Red recombination with pRed/ET (Gene Bridges) and either pBAD-*I-sceI* plasmid (kindly provided by N. Osterrieder, Free University of Berlin, Berlin, Germany) or in *Escherichia coli* strain GS1783 (from G. Smith, Northwestern University, Chicago, IL), as described (3), or by in vitro Gateway (GW) recombination according to the Gateway Technology Manual (Invitrogen). All constructs were confirmed by PCR analysis, field inversion gel electrophoresis analysis of restriction enzyme digests, and targeted DNA sequencing. Targeting plasmids for Red recombination were constructed as described (4). The kanamycin-resistance gene flanked by an I-*Sce*I restriction site (I-*Sce*I-*aphAI* fragment) was amplified from pEPkan-S2 (also from N. Osterrieder, Free University of Berlin, Berlin, Germany) (4) by PCR with the different targeting primers specified below with reference to Table S2. All targeting fragments for Red recombination were purified by a Qiagen gel extraction kit (Qiagen) or SpinSmart Nucleic Acid Prep and Purification Columns (Denville Scientific).

To construct the JΔNI vectors, we first introduced the previously described hyperactive N/T double mutation (5) into the gB gene of KOS-37 BAC and deleted the internal repeat (joint) region. The I-*Sce*I-*aphAI* fragment was cloned into the SnaBI site of plasmid pgB1:D285N/A549T (5). The resulting plasmid, pgB:N/T-kan, was used as a template for amplification with primers R21 and R22, and the product was recombined with the native gB gene of KOS-37 BAC, followed by I-*Sce*I-enhanced deletion of the *aphAI* gene in pBAD-*I-sceI* plasmid-transformed bacteria. Next, we amplified I-*Sce*I-*aphAI* with nested forward primers R6 and R8 and reverse primer R7 for Red-mediated deletion of the joint region (GenBank JQ673480, positions 117,080–132,461), followed by removal of the *aphAI* gene.

Replacement of the ICP4 locus in the joint-deleted gB:N/T BAC with an mCherry expression cassette was achieved as follows. Plasmid pUbC-mCherry-SV40pA was constructed by cloning of the human ubiquitin C promoter (UbCp) from pBluescriptUB-Flag-mArt (a gift from H. Nakai, Oregon Health and Science University, Portland, OR), the mCherry gene from pEP-miR (Cell Biolabs), and the SV40 polyadenylation (polyA or pA) region from pEP4-EO2SCK2M-EN2L (plasmid 20924; Addgene) (6) into pBluescript KS+ (Stratagene). The I-*Sce*I-*aphAI* fragment was then cloned into the BamHI site of pUbC-mCherry-SV40pA at the boundary between UbCp and mCherry to generate pUbC-mCherry-SV40pA-KAN. The insert was PCR-amplified with primers R11 and R12 (Table S2) for Red-mediated recombination with the ICP4 target locus. The resulting construct was deleted for HSV-1 KOS positions 146,113–151,581 of the GenBank JQ673480 sequence, including the TAATGARAT motifs of the ICP22 promoter.

Replacement of the ICP0 and ICP27 IE promoters with the early (β) HSV-1 thymidine kinase (TK) promoter to generate JΔNI2 was initiated by PCR through the TK promoter in front of both the ICP0 and the ICP27 coding region in the JΔββ virus genome (7) with primer pairs R41/42 and R43/44, respectively. The products were cloned into pCRblunt (Invitrogen) to produce pCRBlunt-β0 and pCRBlunt-β27. Insertion of I-*Sce*I-*aphAI* amplified with primer pair R45/46 into the BglII site of pCRBlunt-β0 and with primer pair R47/48 into the HpaI site of pCRBlunt-β27 yielded pCRBlunt-β0-KAN and pCRBlunt-β27-KAN, respectively. The inserts were amplified with primer pairs R41/42 and R43/44, respectively, for Red recombination with the joint-deleted UbCp-mCherry gB:N/T BAC. JΔNI3 was then derived from JΔNI2 by Red-mediated deletion of the complete ICP0 coding sequence using nested targeting forward primers R1 and R2 and reverse primer R3 for I-*Sce*I-*aphAI* amplification. JΔNI5 was likewise derived from JΔNI3 by deletion of the ICP27 coding sequence using primer pair R4/R5 to produce the targeting I-*Sce*I-*aphAI* fragment.

JΔNI6GFP was generated by insertion of an EGFP expression cassette between the UL3 and UL4 genes of JΔNI5. First, plasmid pCAG-GFP was constructed by replacing the gH gene between the CAG promoter (CMV enhancer/chicken-β actin promoter/chimeric intron) and the rabbit β-globin polyA region in plasmid pPEP100 (a gift from P. Spear, Northwestern University, Evanston, IL) (8) with the EGFP gene from pEGFP-C1 (Clontech). I-*Sce*I-*aphAI* was then inserted into the SnaBI site of pCAG-GFP to create plasmid pCAG-GFPKAN. Separately, multistep PCR using KOS-37 BAC DNA as initial template was performed to generate a fragment that contained multiple new cloning sites (MCS) between the UL3 and UL4 polyA regions, as follows. First, extension PCR was performed to amplify the 3′ UTRs of UL3 and UL4 with primer pairs R17/18 and R19/20, respectively, that added an overlapping MCS region to each 3′ UTR fragment. The two PCR products were gel-purified, and 100 ng of each was used for overlapping PCR with primers R17 and R19 to create a continuous fragment. This product was cloned into pCRBlunt (Invitrogen), yielding plasmid pCRBluntUL3-4linker. The insert of pCAG-GFPKAN was then cloned between the AccI and PsiI sites in the MCS of pCRBluntUL3-4linker. The resulting plasmid was digested with MfeI and PpuMI, and the UL3-CAG-GFPKAN-UL4 fragment was isolated for recombination with the UL3-UL4 intergenic region of JΔNI5 followed by *aphAI* gene removal.

To create JΔNI7GFP, an XhoI fragment (~6.2 kb) containing the two CTRLs, LAP1 and LATP2, of the HSV-1 LAT locus was isolated from KOS-37 BAC DNA and cloned into pBluescript

KS+. An internal KpnI-SalI fragment extending from near the end of LATP2 to ~250 bp downstream of CTRL2 was isolated from this recombinant and cloned between the KpnI and SalI sites of pSP72 (Promega) to produce pSP72KOS-LAT. An MCS was then introduced between two BstXI sites located ~240 and ~430 bp downstream of the KpnI site, yielding pSP72KOS-LATlinker. Separately, plasmid pCAG-GW was constructed by replacing the gH gene of pPEP100 with a PCR-amplified modified GW recombination cassette (GW-Zeo; zeocin resistance instead of chloramphenicol resistance) (9). The insert of pCAG-GW was then cloned into the MCS of pSP72KOS-LATlinker to produce pSP72KOS-LATlinker-CAG-GW. The plasmid was digested with KpnI and HpaI to isolate the CAG-GW region with flanking LAT sequences for Red-mediated recombination with the LAT locus of JΔNI5 in *ccdB*-resistant HerpesHogs bacteria (9). Finally, the GW cassette in the resulting JΔNI5 recombinant BAC was replaced with the EGFP gene by Red-mediated recombination with an AatII-PsiI fragment, including CAG and polyA sequences, of plasmid pCAG-GFPKAN. JΔNI7GFP derivatives deleted for specific LAT region elements outside the EGFP cassette (CTRL1, GenBank JQ673480, positions 8,978–9,161; CTRL2, positions 5,694–5,857; LATP2, positions 6,123–7,530) were generated by Red-mediated recombination of JΔNI7GFP DNA with targeted I-*SceI*-*aphAI* cassettes produced by PCR with the respective F1, F2, and R primers listed in Table S2.

For the construction of the different JΔNI9 and JΔNI10 vectors, the remainder of the LAT region, including CTRL1, LATP2, and CTRL2, was deleted from the JΔNI5 genome by recombination with LAT-targeted I-*SceI*-*aphAI* generated by PCR with primers R38, R39, and R40, producing JΔNI5ΔL. GW-Zeo was then amplified with targeting primers for the intergenic region between UL45 and UL46 (R34/35) or UL50 and UL51 (R36/37), and the product of each reaction was recombined with JΔNI5ΔL BAC DNA to create JΔNI9GW and JΔNI10GW. JΔNI7GFP BAC DNA was digested with XhoI, and the ~7.2-kb CAG-GFP-containing fragment from the LAT locus was isolated and cloned into pENTR1A (pENTR-LAT-XhoI). The corresponding ~5.3-kb XhoI fragment of JΔNI7GFPΔC12LP2 was likewise isolated and cloned into pENTR1A (pENTR-LATΔ-XhoI), and, lastly, the insert of pCAG-GFP (see above) was transferred into pENTR1A (pENTR-CAG-GFP). In vitro LR Clonase (Invitrogen) reactions were then performed to recombine the different pENTR constructs with JΔNI10GW BAC DNA, producing JΔNI10LAT-GFP, JΔNI10ΔC12LP2-GFP, and JΔNI10GFP, respectively, and pENTR-LAT-XhoI and pENTR-CAG-GFP were recombined with JΔNI9GW BAC DNA to generate JΔNI9LAT-GFP and JΔNI9GFP.

For the construction of JΔNI7-GWL1, the GW-Zeo cassette was amplified with primers R49 and R50 and cloned into the MCS of pSP72KOS-LATlinker to create pSP72KOS-LATlinker-GW. The GW region with flanking homology arms was isolated by digestion with KpnI and HpaI and recombined with the LAT locus of JΔNI5 by Red-mediated recombination.

JΔNI7mDMD was derived from JΔNI7-GWL1. We first constructed plasmid pENTR-CAG-mcs-β-globin polyA by replacement of the EGFP gene-containing EcoRI/BglII fragment of pENTR-CAGGFP with a synthetic MCS. A full-length mouse dystrophin cDNA was then obtained from plasmid pCCL-DMD (10) (a kind gift from C. T. Caskey, Baylor College of Medicine, Houston, TX) by NotI digestion and cloned into the NotI site in the MCS of pENTR-CAG-mcs-β-globin polyA to generate pENTR-CAGmDMD (Fig. S6). Gateway LR recombination of pENTR-CAGmDMD with JΔNI7-GWL1 was then used to produce JΔNI7mDMD.

KNTc was constructed by introduction of the gB:N/T mutations into KOS-37 BAC as described above, and the UbCp-mCherry cassette into the intergenic region between UL3 and UL4 by Red recombination with the insert of pUbC-mCherry-SV40pA-KAN targeted by amplification with primers R13 and R14.

Viruses. JΔNI BAC DNAs were converted to infectious viruses by transfection of U2OS-based complementing cells. DNA in 500 μL of OptiMEM (Invitrogen) was incubated with 1 μL of Lipofectamine Plus Reagent (Invitrogen) for 5 min at room temperature, 6.25 μL of Lipofectamine LTX (Invitrogen) was added, and the mixture was incubated for 30 min at room temperature and added to cells. After incubation at 37 °C for 6 h, the transfection mix was removed, and the cells were cultured overnight at 37 °C with serum-free DMEM, transferred to a 33 °C incubator, and monitored for 100% cytopathic effect (CPE). Supernatants were titered and then amplified by infection of sequentially larger cultures at an MOI of 0.001 pfu per cell. KNTc infectious virus was produced by transfection of Vero cells using 3 μL of Lipofectamine Plus Reagent and 9 μL of Lipofectamine LTX for 4 h at 37 °C; an MOI of 0.01 pfu per cell was used for KNTc virus amplification on Vero cells. Complementing cells for transfections and/or virus growth were as follows: U2OS-ICP4 (JΔNI2, JΔNI3), U2OS-ICP4/27 (JΔNI5 and derivatives), and Vero-7b (QOZHG virus). All virus stocks were titered on U2OS-ICP4/27 cells (Table 2). Physical titers [genome copies (gc)/mL] were determined by quantitative real-time PCR as described below. Fluorescent images of infected cells were obtained with a Nikon Diaphot fluorescence microscope (Nikon) at 40× magnification or at 100× magnification (Fig. S3*A* only).

Virus Growth Curves. Replicate wells of Vero-7b, U2OS, U2OS-ICP4, and U2OS-ICP4/27 cells in a 24-well plate were infected at an MOI of 0.001 for 2 h, treated with 0.1 M glycine (pH 3.0) for 1 min to inactivate extracellular virus, and incubated at 37 °C and 5% CO_2. Media were harvested daily and titered by standard plaque assay on U2OS-ICP4/27 cells.

Cytotoxicity Assay. HDF and Vero cells (5×10^3) were seeded in a 96-well plate and infected at 25,000 gc per cell. Cell viabilities were determined at 1–3 or 5 dpi by MTT assay, essentially as described (11).

Western Blotting and Immunofluorescence. Cell lysate preparation and Western blotting were typically performed as described (12). For Western blotting of dystrophin, cell lysates were separated on NuPAGE Novex 3–8% Tris-Acetate Protein Gels (Invitrogen). Polyclonal rabbit anti-ICP0 antibodies were produced in our laboratory, anti-ICP27 (10-H44) was from Fitzgerald Industries International (www.fitzgerald-fii.com), anti-ICP22 was a gift from John Blaho (Mount Sinai School of Medicine, New York), anti-ICP4 (10F1) was from Santa Cruz Biotechnology, anti–α-tubulin (T6793) was from Sigma, and anti-dystrophin was from Millipore (clone 1808). Immunofluorescence using the same ICP4, ICP27, and dystrophin antibodies or anti-Cre antibody 2D8 (Millipore) was performed essentially as described (13) and was recorded under a Zeiss axiovert 200 fluorescence microscope (Zeiss) (anti-dystrophin) or a Nikon Diaphot fluorescence microscope (all others) at 100× magnification.

Quantitative Reverse Transcription-PCR and Genome PCR. For qRT-PCR, total RNA was typically extracted using an RNeasy kit (Qiagen). cDNA was synthesized with a RETROscript Kit (Ambion). Real-time PCR was carried out in triplicate by the StepOnePlus Real-Time PCR System (Applied Biosystems). For small numbers of cells, a Cells-to-cDNA II Kit (Ambion) was used for cell lysis and reverse transcription. Results for 18S ribosomal (r) RNA or viral particle number were used to normalize the data. All qRT-PCR primers used in this study are listed in Table S3 (Q1–Q36).

For the determination of physical (genome copy) titers of virus stocks, 5 μL of virus was incubated with 300 U/mL Benzonase nuclease (Sigma) for 1 h at 25 °C in the presence of 2 mM $MgCl_2$, and viral DNA was extracted by a DNeasy Blood and Tissue Kit (Qiagen). Then, gc titers were determined by qPCR for the glycoprotein D (gD) gene with the gD primers (Q37, Q38) and probe (Q39) listed in Table S3. Amounts of nuclear viral DNA were determined by rinsing the cells at 2 hpi, isolation of nuclei as described (14, 15), DNA extraction with the DNeasy Blood and Tissue Kit, and qPCR for the gD gene as above. Cellular 18S ribosomal DNA levels were measured with the use of TaqMan Ribosomal RNA Control Reagents (Invitrogen) and were used to normalize viral DNA amounts.

Generation of U2OS-ICP4/27-Cre Cells. Retroviral expression plasmid pCX4Hyg-Cre for stable Cre expression in U2OS-ICP4/27 cells was constructed as follows. A PCR-amplified Gateway recombination cassette (12) was inserted into the multicloning site of pCX4Hyg (a kind gift from T. Akagi, KAN Research Institute, Kobe, Japan; GenBank accession no. AB086387) to create plasmid pCX4Hyg-GW. The complete NLS-Cre coding sequence from plasmid pTurbo-Cre (ES Cell Core; Washington University School of Medicine; GenBank accession no. AF334827.1) was inserted between the *att*L1 and *att*L2 sites of pENTR1A (Invitrogen) and then transferred into pCX4Hyg-GW by LR Clonase-mediated Gateway recombination, creating pCX4Hyg-Cre. Retroviral particles were produced as described (16). Briefly, 293T cells were cotransfected with pCX4Hyg-Cre, pCL-GagPol, and pHCMV-VSV-G vectors (the last two kindly provided by N. Kiyokawa, H. Okita, and A. Umezawa, NRICHD, Tokyo), supernatant was collected 48 h later, filtered through a 0.45-μm filter, and concentrated by centrifugation. U2OS-ICP4/27 cells were infected with the purified Cre retrovirus and selected for resistance to puromycin (2 μg/mL), blasticidin (10 μg/mL), and hygromycin (200 μg/mL). Resistant clones were isolated and screened for Cre expression by immunostaining with anti-Cre antibody 2D8 (Millipore).

BAC Excision. BAC-deleted viruses (JΔNI5ΔB, JΔNI7GFPΔB, JΔNI7mDMDΔB) were generated by infection of U2OS-ICP4/27-Cre cells with JΔNI5, JΔNI7GFP, or JΔNI7mDMD virus at 0.001 gc per cell. At 100% CPE, supernatants were harvested and cleared, and individual recombinants were isolated by standard limiting dilution (17) on U2OS-ICP4/27 cells. Viruses were screened for loss of β-galactosidase activity by infection of U2OS-ICP4/27 cells at 10 gc per cell and X-gal staining (17) 48 h later. Accurate BAC deletion was confirmed by PCR across the remaining loxP site and sequencing of the product.

Statistics. All values are presented as the mean ± SD. Differences between pairs were analyzed by Student's *t* test using Microsoft Excel 14.4.1. *P* values below 0.05 ($P < 0.05$) were considered statistically significant.

1. Rasty S, Poliani PL, Fink DJ, Glorioso JC (1997) Deletion of the S component inverted repeat sequence c' and the nonessential genes U(S)1 through U(S)5 from the herpes simplex virus type 1 genome substantially impairs productive viral infection in cell culture and pathogenesis in the rat central nervous system. *J Neurovirol* 3(4):247–264.
2. Gierasch WW, et al. (2006) Construction and characterization of bacterial artificial chromosomes containing HSV-1 strains 17 and KOS. *J Virol Methods* 135(2):197–206.
3. Tischer BK, Smith GA, Osterrieder N (2010) En passant mutagenesis: A two step markerless red recombination system. *Methods Mol Biol* 634:421–430.
4. Tischer BK, von Einem J, Kaufer B, Osterrieder N (2006) Two-step red-mediated recombination for versatile high-efficiency markerless DNA manipulation in Escherichia coli. *Biotechniques* 40(2):191–197.
5. Uchida H, et al. (2010) A double mutation in glycoprotein gB compensates for ineffective gD-dependent initiation of herpes simplex virus type 1 infection. *J Virol* 84(23):12200–12209.
6. Yu J, et al. (2009) Human induced pluripotent stem cells free of vector and transgene sequences. *Science* 324(5928):797–801.
7. Craft AM, et al. (2008) Herpes simplex virus-mediated expression of Pax3 and MyoD in embryoid bodies results in lineage-Related alterations in gene expression profiles. *Stem Cells* 26(12):3119–3129.
8. Pertel PE, Fridberg A, Parish ML, Spear PG (2001) Cell fusion induced by herpes simplex virus glycoproteins gB, gD, and gH-gL requires a gD receptor but not necessarily heparan sulfate. *Virology* 279(1):313–324.
9. Wolfe D, Craft AM, Cohen JB, Glorioso JC (2010) A herpes simplex virus vector system for expression of complex cellular cDNA libraries. *J Virol* 84(14):7360–7368.
10. Lee CC, Pearlman JA, Chamberlain JS, Caskey CT (1991) Expression of recombinant dystrophin and its localization to the cell membrane. *Nature* 349(6307):334–336.
11. Uchida H, et al. (2013) Novel mutations in gB and gH circumvent the requirement for known gD Receptors in herpes simplex virus 1 entry and cell-to-cell spread. *J Virol* 87(3):1430–1442.
12. Miyagawa Y, et al. (2009) EWS/ETS regulates the expression of the Dickkopf family in Ewing family tumor cells. *PLoS ONE* 4(2):e4634.
13. Uchida H, et al. (2009) Generation of herpesvirus entry mediator (HVEM)-restricted herpes simplex virus type 1 mutant viruses: Resistance of HVEM-expressing cells and identification of mutations that rescue nectin-1 recognition. *J Virol* 83(7):2951–2961.
14. Dignam JD, Lebovitz RM, Roeder RG (1983) Accurate transcription initiation by RNA polymerase II in a soluble extract from isolated mammalian nuclei. *Nucleic Acids Res* 11(5):1475–1489.
15. Suzuki K, Bose P, Leong-Quong RY, Fujita DJ, Riabowol K (2010) REAP: A two minute cell fractionation method. *BMC Res Notes* 3:294.
16. Makino H, et al. (2009) Mesenchymal to embryonic incomplete transition of human cells by chimeric OCT4/3 (POU5F1) with physiological co-activator EWS. *Exp Cell Res* 315(16):2727–2740.
17. Goins WF, et al. (2002) Construction of replication-defective herpes simplex virus vectors. *Curr Protoc Hum Genet* 33:12.11:12.11.1–12.11.30.

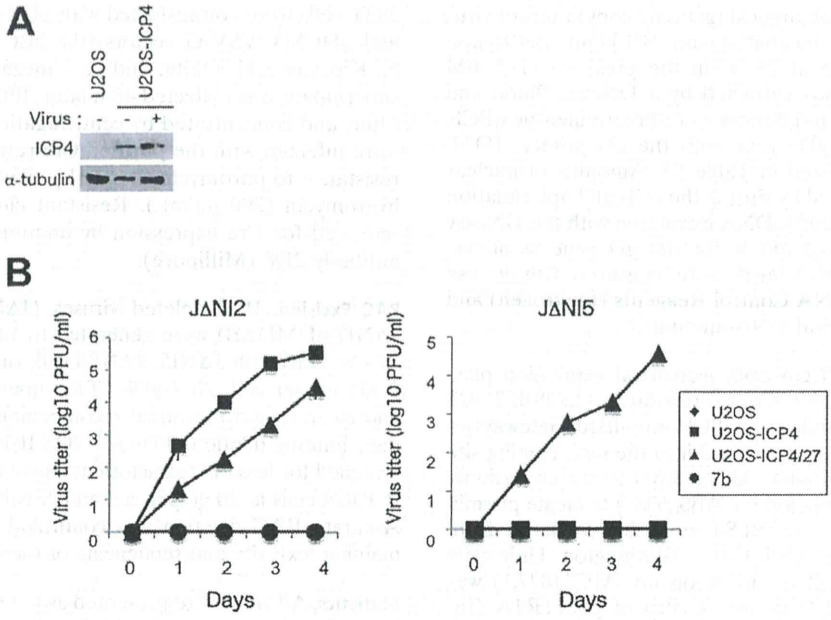

Fig. S1. U2OS-ICP4 cells and complementation requirements for JΔNI2 and JΔNI5 growth. (*A*) Western blot analysis of U2OS-ICP4 cells. Uninfected cells and cells infected with ICP4-deficient QOZHG virus (1) at an MOI of 1 were harvested at 24 hpi, and extracts were prepared for gel electrophoresis; an extract from uninfected U2OS cells was included as a control. The blot was probed with antibodies for ICP4 or α-tubulin as a loading control. The results show that ICP4 expression is independent of induction by virus infection. (*B*) JΔNI2 (*Left*) and JΔNI5 (*Right*) virus growth in U2OS, U2OS-ICP4, U2OS-ICP4/27, and Vero-7b (2) cells. Cells were infected at an MOI of 0.001, and extracellular virus from duplicate wells ($n = 2$) was harvested daily and titered on U2OS-ICP4/27 cells.

1. Chen Xp, et al. (2000) Herpes simplex virus type 1 ICP0 protein does not accumulate in the nucleus of primary neurons in culture. *J Virol* 74(21):10132–10141.
2. Krisky DM, et al. (1998) Deletion of multiple immediate-early genes from herpes simplex virus reduces cytotoxicity and permits long-term gene expression in neurons. *Gene Ther* 5(12): 1593–1603.

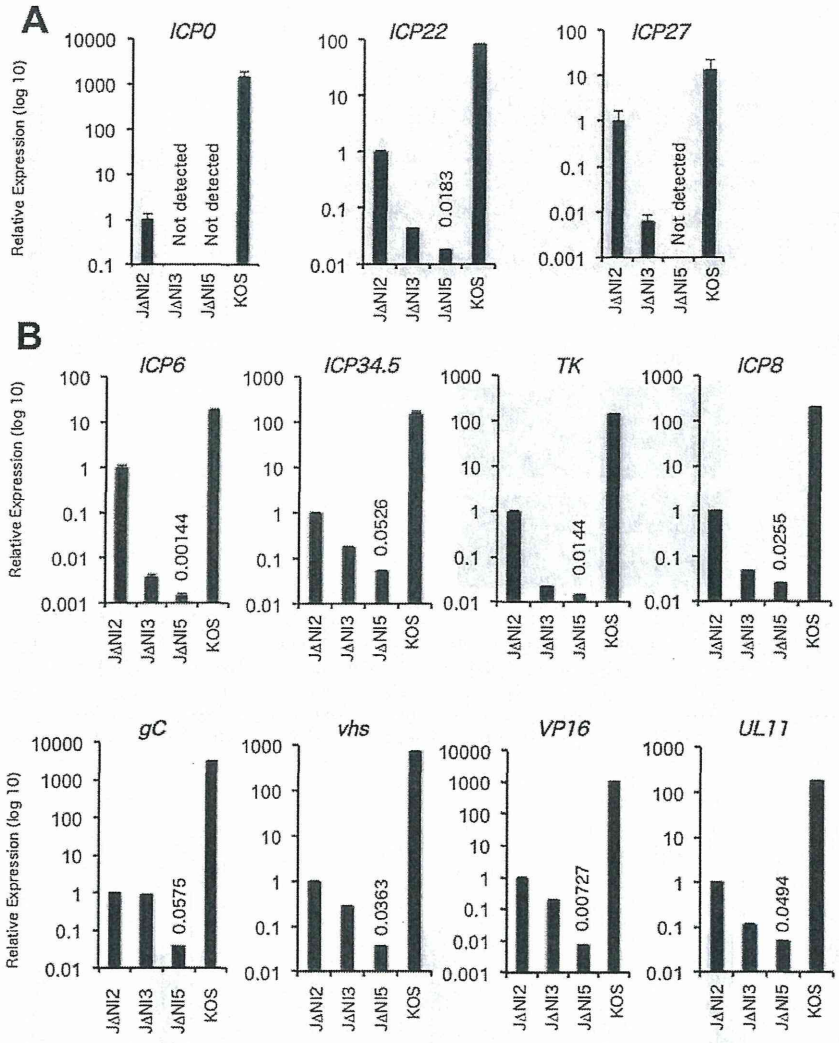

Fig. S2. JΔNI viral gene expression in noncomplementing cells. (*A*) JΔNI IE gene expression measured by qRT-PCR. HDFs were infected with the indicated viruses at 1,000 gc per cell. mRNA was isolated at 12 hpi and reverse-transcribed for qPCR determination of the cDNA levels for the genes listed at the top. Expression was normalized to 18S rRNA levels and is shown relative to JΔNI2-infected cells. (*B*) qRT-PCR analysis for expression of early (*Upper*) and late genes (*Lower*). HDFs were infected and processed as in *A*. ICP6 may be considered a delayed IE gene and is grouped here with the early genes because its expression is reportedly more dependent on ICP0 than on VP16 (1, 2). Data in *A* and *B* represent averages ± SD of two independent experiments.

1. Desai P, et al. (1993) The RR1 gene of herpes simplex virus type 1 is uniquely trans activated by ICP0 during infection. *J Virol* 67(10):6125–6135.
2. Sze P, Herman RC (1992) The herpes simplex virus type 1 ICP6 gene is regulated by a 'leaky' early promoter. *Virus Res* 26(2):141–152.

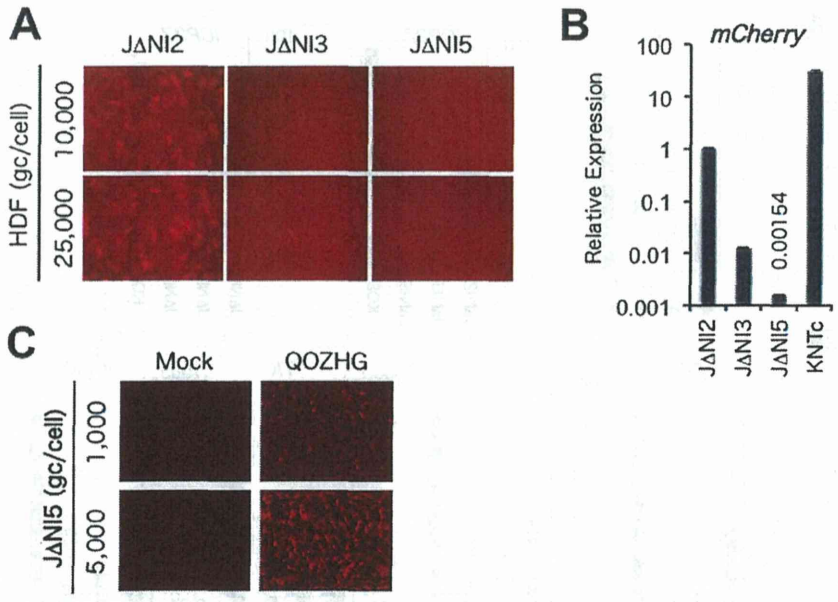

Fig. S3. Reporter-gene expression in JΔNI-infected HDFs. (*A*) mCherry fluorescence in infected HDFs. Cells were infected at the indicated gc per cell and photographed at 24 hpi and 100× magnification. (*B*) Relative mCherry mRNA levels in HDFs. Cells were infected at 5,000 gc per cell and harvested at 6 hpi for mRNA isolation and qRT-PCR with mCherry-specific primers listed in Table S3. Expression was normalized to 18S rRNA levels and is shown relative to JΔNI2-infected cells (averages ± SD of two independent experiments). KNTc is a replication-competent control vector that contains a UbC promoter-mCherry expression cassette in the intergenic region between the U_L3 and U_L4 genes and the entry-enhancing N/T double mutation in gB (5). (*C*) Induction of mCherry expression in JΔNI5-infected HDFs. Cells were infected at the indicted gc per cell, superinfected at 24 h with QOZHG at 5,000 gc per cell, and photographed 24 h later at 40× magnification.

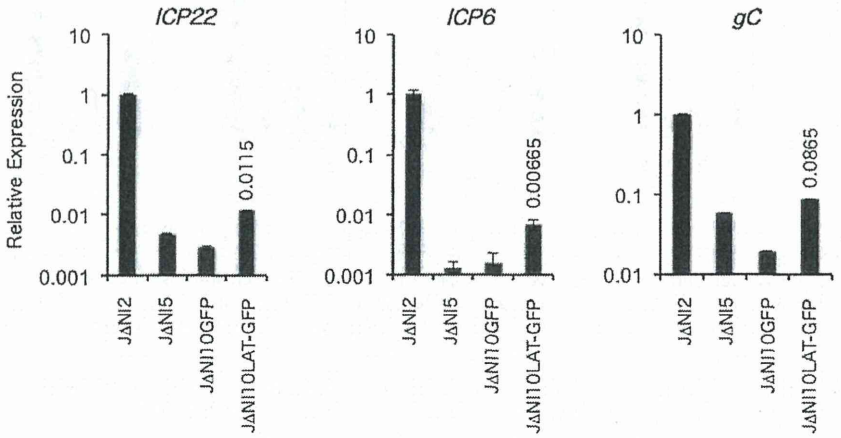

Fig. S4. Effect of repositioned LAT elements on viral gene expression. HDFs were infected with the indicated viruses at 1,000 gc per cell. mRNA was isolated at 12 hpi and reverse-transcribed for qPCR determination of the cDNA levels for the genes listed at the top. Expression was normalized to 18S rRNA levels and is shown relative to JΔNI2-infected cells (averages of two independent experiments ± SD).

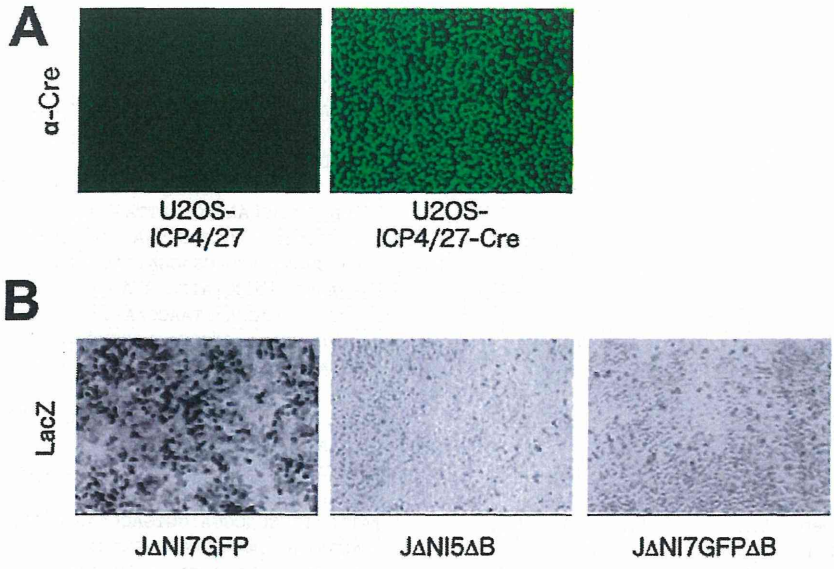

Fig. S5. Cre-expressing complementing cell line and its utilization for BAC excision. (*A*) Confirmation of Cre expression in U2OS-ICP4/27-Cre cells by anti-Cre immunofluorescent staining in comparison with the parental U2OS-ICP4/27 cell line. (*B*) Loss of *lacZ* gene expression after virus passage through U2OS-ICP4/27-Cre cells. Representative images of β-galactosidase activity in U2OS-ICP4/27 cells infected with JΔNI7GFP virus (BAC+) or U2OS-ICP4/27-Cre–passaged (BAC-excised) virus isolates (Δ*B*). Cells were infected at 10 gc per cell, fixed 48 h later, and stained with X-gal (dark cells).

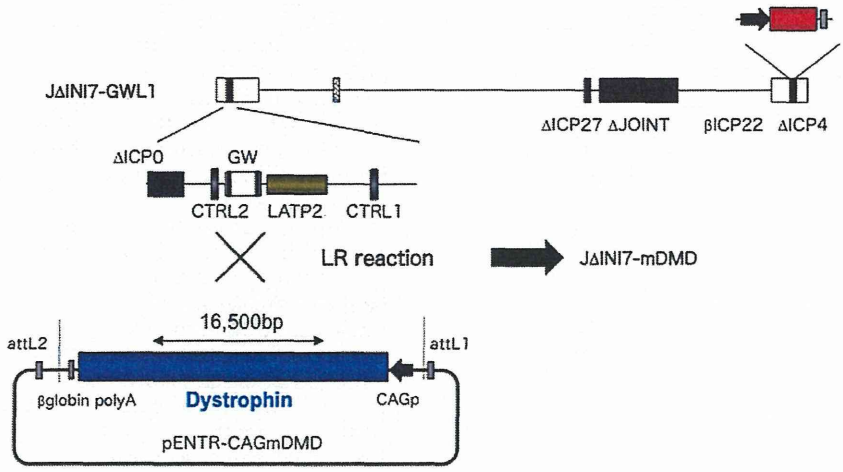

Fig. S6. Construction of vector JΔNI7mDMD. Red-mediated recombination was used to introduce a Gateway cassette between LATP2 and CTRL2 of JΔNI5, creating JΔNI7-GWL1 (*Upper*). A 16.5-kb expression cassette for full-length mouse dystrophin consisting of the CAG promoter, the complete mouse dystrophin cDNA, and the rabbit β-globin polyA region was assembled in a pENTR plasmid (*Lower*) and transferred into the LAT region of JΔNI7-GWL1 by GW recombination ("LR reaction") to generate JΔNI7mDMD.

Table S1. JΔNI5 plaquing efficiency on U2OS-ICP4/27 cells at different passage numbers

Passage no.	Plaque no. (mean ± SD)
p5	17.33 ± 6.35
p10	15 ± 2.64
p20	16 ± 4

U2OS-ICP4/27 cells were infected with JΔNI5 virus at 0.1 gc per cell, and the cells were overlayed with methylcellulose at 2 hpi. Plaques were counted at 4 dpi. Means ± SD of three determinations.